Scientific Research Publishing

Modeling and Numerical Simulation of Material Science, 2022, 12, 13-23
https://www.scirp.org/journal/mnsms
ISSN Online: 2164-5353
ISSN Print: 2164-5345

Simulation of a CIGS Solar Cell with $CIGSe_2/MoSe_2/Mo$ Rear Contact Using AFORS-HET Digital Simulation Software

Donafologo Soro[1*], Adama Sylla[2], N'Guessan Armel Ignace[2], Aboudoulaye Toure[3], Amal Bouich[3], Siaka Toure[2], Bernabé Marí[3]

[1]Department of Science and Technology, Ecole Normale Supérieure (ENS) of Abidjan, Abidjan, Ivory Coast
[2]Solar Energy Laboratory, FHB University of Abidjan-Cocody, Abidjan, Ivory Coast
[3]Department ofApplied Physics-IDF, Polytechnic University of Valencia, Valencia, Spain
Email: *donafologosoro@yahoo.fr

How to cite this paper: Soro, D., Sylla, A., Ignace, N.A., Toure, A., Bouich, A., Toure, S. and Marí, B. (2022) Simulation of a CIGS Solar Cell with $CIGSe_2/MoSe_2/Mo$ Rear Contact Using AFORS-HET Digital Simulation Software. *Modeling and Numerical Simulation of Material Science*, **12**, 13-23.
https://doi.org/10.4236/mnsms.2022.122002

Received: December 14, 2021
Accepted: March 12, 2022
Published: March 15, 2022

Abstract

In this work, the AFORS-HET digital simulation software was used to calculate the electrical characteristics of the cell/n-ZnO/i-ZnO/n-Zn (O, S)/p-$CIGSe_2$/p + -$MoSe_2$/Mo/SLG. When the thickness of the $CIGSe_2$ absorber is between 3.5 and 1.5 µm, the efficiency of the cell with an interfacial layer of $MoSe_2$ remains almost constant, with an efficiency of about 24.6%, higher to that of a conventional cell which is 23.4% for a thickness of 1.5 µm of $CIGSe_2$. To achieve the expected results, the $MoSe_2$ layer must be very thin less than or equal to 30 nm. In addition, a Schottky barrier height greater than 0.45 eV severely affects the fill factor and the open circuit voltage of the solar cell with $MoSe_2$ interface layer.

Keywords

CIGS, Molybdenum Diselenide ($MoSe_2$), AFORS-HET, Simulation, Efficiency

1. Introduction

Global energy needs are mainly based on the exploitation of energies fossils and fissiles (petroleum, natural gas, coal, uranium, etc.). At the rate of current energy consumption, a depletion of available resources is expected in less than three half centuries [1]. In addition, soaring costs, the fight against greenhouse gas emissions and the concept of sustainable development make the consumption and diversification of new so-called clean energy sources urgent. The use and development of renewable energies therefore appear to be a means that would contribute to the healthy satisfaction of the planet's energy needs in this context of diversification of energy resources and especially of sustainable development. The development of the generation of photovoltaic cells based on Cu (In, Ga) Se_2 suggests many advantages at the environmental and economic levels. They have many advantages, such as high conversion efficiency, high stability, low cost, and adjustable bandgap. Cu (In, Ga) Se_2 has become one of the most promising materials for thin film solar cells.

CIGSe-based high efficiency solar cells have been the subject of many years of theoretical and experimental research. Several researchers have demonstrated the efficiency of CIGS solar cells greater than 21%. Solibro achieved 21% efficiency, the Solar Energy and Hydrogen Research Center and Solar Frontier claim 21.7% and 22.3% efficiencies respectively, but these values reported as exceptions [2] [3] [4] [5] [6] remain quite close to the result obtained from the crystalline silicon solar cell which is about 25% [7].

In addition to these technological advances observed, significant efforts have been devoted to understanding the physical properties of the key material of these cells, namely the CIGSe absorbent layer. Indeed, the performance of these cells largely depends on the physical properties of the CIGSe alloys which are not yet fully clarified. These include the nature and energy levels of CIGSe absorbent layer defects and buffer/absorber interface defects.

One of the challenges is to drastically reduce the thickness of the $CIGSe_2$ absorber. In this case, the rate of photogeneration of the carriers near the rear contact can no longer be negligible and the rate of recombination at the rear interface is essential. Another approach is to create an electric field inside the absorber by gradation of the band gap located in the appropriate regions. This results in various cellular structures with different CIGS composition profiles: the "front grading" which has a higher bandgap towards the buffer layer, the "back grading" which has a higher bandgap towards the rear contact layer and the "double grading" which combines the first two gradation profiles. Thus, the forward gradation reduces recombination at the buffer/absorber junction and the rear gradation is near the rear side pushing the minority carriers towards the collector junction, then reducing the recombination of carriers at the rear of the absorber [8].

The aim of this work is therefore to analyze the influence of the interfacial layer of $MoSe_2$ on the performance of a solar cell/n-ZnO/i-ZnO/n-Zn (O, S)/ p-$CIGSe_2$/p + -$MoSe_2$/Mo/SLG.

2. Numerical Modelling and Device Simulation

To understand the influence of the rear contact on the performance of the cell in the case where a $MoSe_2$ layer is inserted between the absorber and the rear Mo: $CIGSe_2$/$MoSe_2$/Mo contact, calculations are carried out using the software of numerical simulation AFORS-HET (Automate FOR Simulation of HETero-structures) developed by the Helmholtz-Zentrum-Berlin (HZB) laboratory since 2000 [9] for the modeling of homo- or heterojunction multilayer solar cells. It solves, by the finite difference method, the Poisson, continuity equations for electrons and one-dimensional holes at thermodynamic equilibrium given respectively by R. Varache [9].

$$-\varepsilon_0\varepsilon_r \frac{\partial^2 V(x,t)}{\partial^2 x} = q\left[p(x,t)-n(x,t)+N_D(x)-N_A(x)\right]+\sum_{piege}\rho_{piege} \tag{1}$$

$$-\frac{1}{q}\frac{\partial J_n(x,t)}{\partial x} = G(x,t)-R_n(x,t)-\frac{\partial n(x,t)}{\partial t} \tag{2}$$

$$\frac{1}{q}\frac{\partial J_p(x,t)}{\partial x} = G(x,t)-R_p(x,t)-\frac{\partial \rho(x,t)}{\partial t} \tag{3}$$

where ε_r and ε_0 are respectively the relative dielectric constants and vacuum, V the electric potential, p and n the densities of carriers, N_A and N_D the concentrations of acceptor and donor atoms, J_n and J_p the current densities of electrons and holes, G and R_p, n are the rate of generation and recombination of holes and electrons respectively. To these equations, we add the one-dimensional transport equations which express the current density for each type of carrier:

$$J_n = q\mu_n n(x)\varepsilon + qD_n\frac{dn(x)}{dx} \tag{4}$$

$$J_p = q\mu_p p(x)\varepsilon + qD_p\frac{dn(x)}{dx} \tag{5}$$

3. Presentation of the AFORS-HET Software

The AFORS-HET digital simulator can be used to achieve several types of results, among others, the JV characteristic, the external (EQE) and internal (IQE) quantum yields, the capacitance-voltage (CV), capacitance-frequency (Cf) and temperature capacity (CT). A graphical interface makes possible to visualize, store and compare all the simulated data. It is therefore an intermediate tool between the theoretical model and experience. It thus makes it possible to translate the physical reality by taking into account the various constraints linked to the physical phenomena which intervene in the operation of the device or the associated mathematical models which link all the variables. The operation of the device can be simulated under voltage, direct current (DC), transient or weak sinusoidal modulation (AC) and/or under lighting. The handling of this simulator is quite easy because it has an intuitive graphical interface which allows to define the solar cell structures (assembly of layers) and to control the physical parameters. This interface is divided mainly into three areas which are; the main program control panel, the external parameters panel and the measurements panel (**Figure 1**).

3.1. The Main Program Control Panel

This is the area where we can define the structure to be simulated and the parameters of each layer of material used (thickness, dielectric constant, gap, electron affinity, mobility, density of effective states, doping, absorption coefficient, energy level of defects, density of defects). It is possible to define from the "define structure" tab, the type of fault distribution and the effective capture section (Figure 2 and Figure 3). This panel also allows the mesh of the cell for a more precise calculation.

3.2. External Settings Panel

It is used to define the external parameters such as the temperature, the illumination spectrum and the range of variation of the voltage or current of the cell Figure 1.

3.3. Measurements Panel

This is the area that allows the variations in characteristic (J-V) and quantum efficiency (EQE) to be numerically assessed. It also makes possible to choose the measurement to be carried out, for example curve I-V, EQE, IQE, the surface photo-tension according to the tension (VD-SPV, etc.) Figure 1.

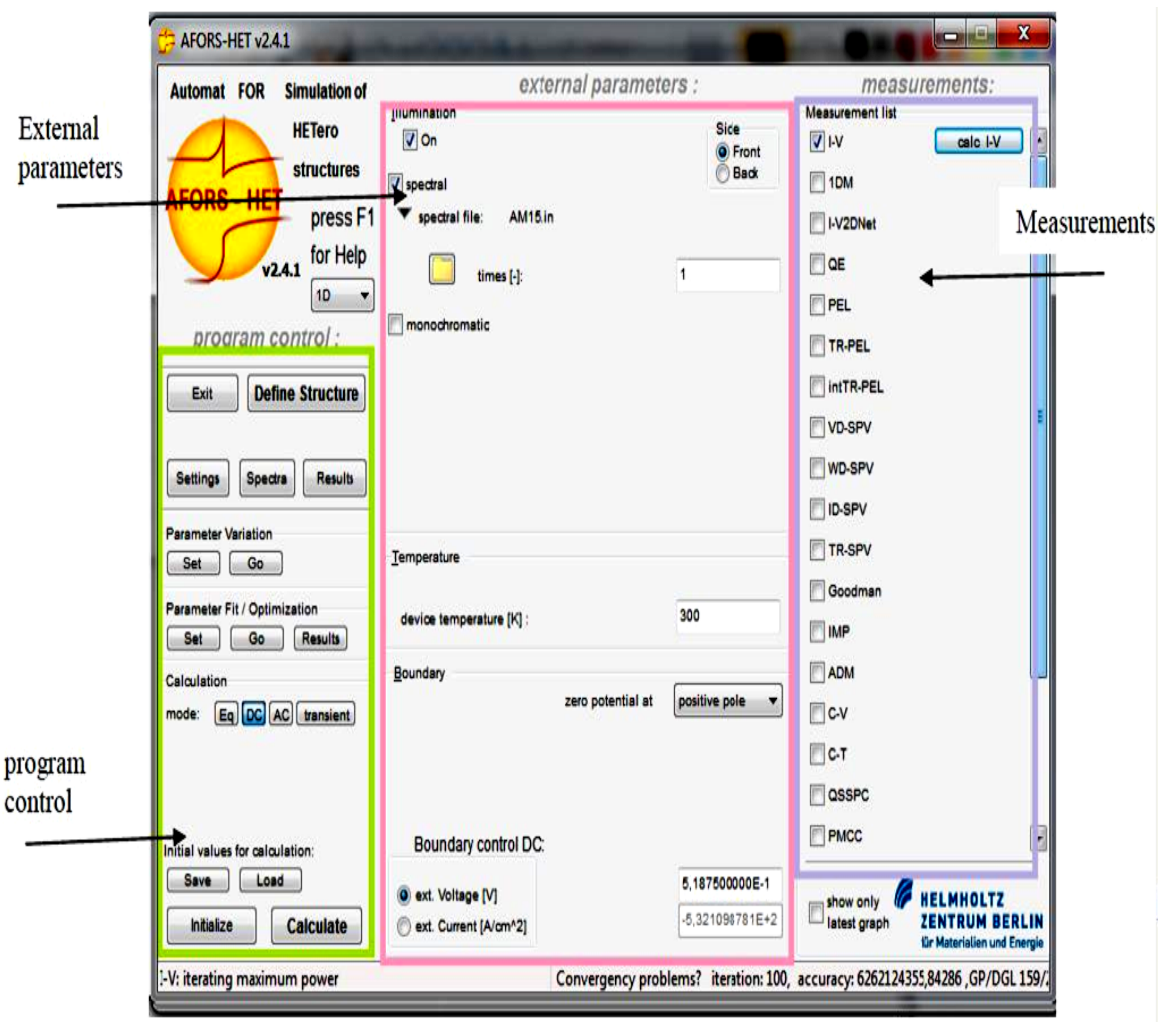

Figure 1. Interface graphique du simulateur numérique AFORS-HET.

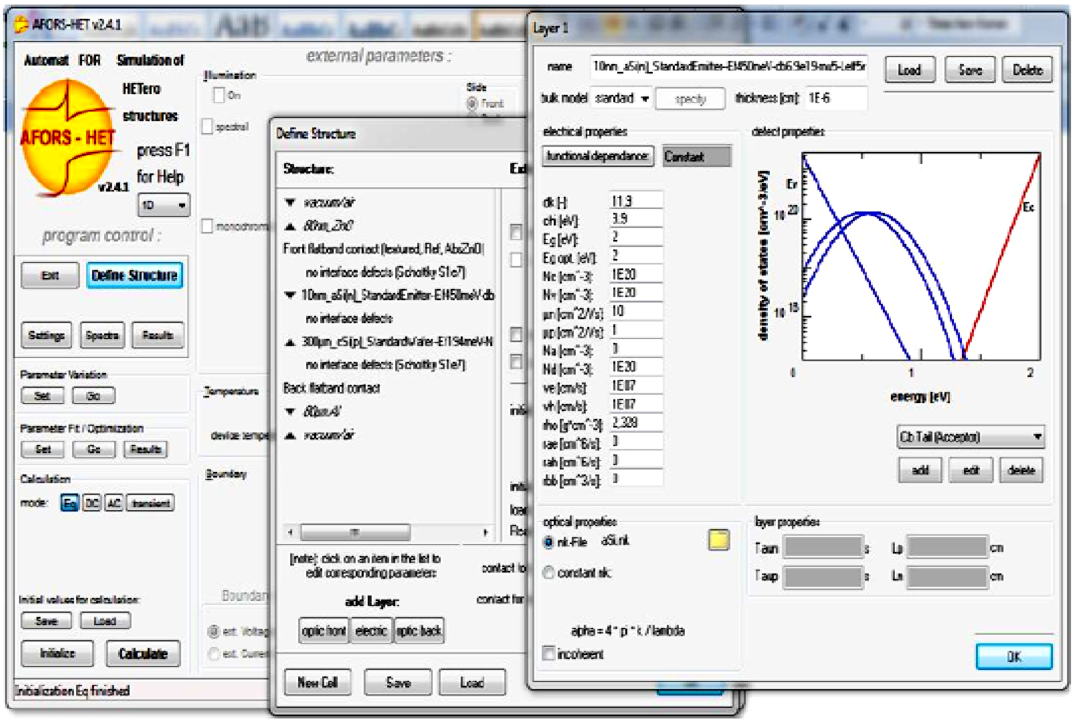

Figure 2. Definition of the structure and the layers parameters.

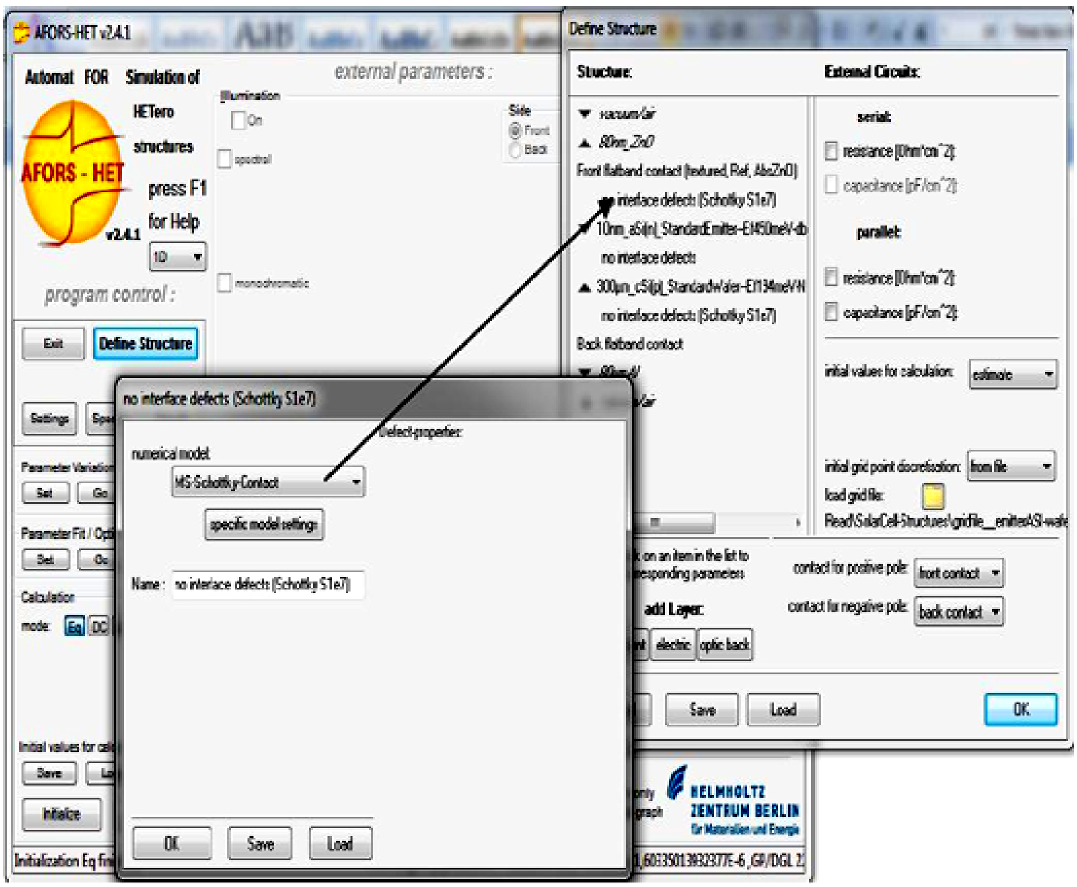

Figure 3. Choice of interface between two layers.

4. Material Properties

CIGS polycrystalline solar cells are made up of several different layers. Numerical values or material properties cannot be derived directly from the theoretical concept. To perform a simulation, you always have to start from a basic structure. By performing a simulation, the quantitative analysis on the performance parameters and behavior of the cell can be studied. It is possible to determine the relationship between the performance parameters that influence the performance or behavior of the solar cell [10]. **Figure 4** shows the structures of the cell to be simulated with a thin layer of $MoSe_2$ at the contact interface. $pCIGSe_2$/$pMoSe_2$/Mo and the parameters which were used for the simulation of our cells are listed in **Table 1**.

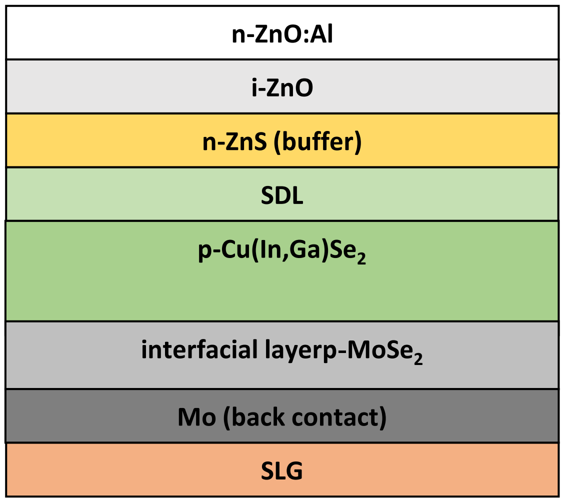

Figure 4. Structure of the CIGS solar cell with a $MoSe_2$ layer at the rear contact interface.

Table 1. Simulation input parameters.

Parameters	$MoSe_2$	$CIGSe_2$	SDL	ZnS	i-ZnO	ZnO:Al
Thickness (μm)	0.03	1.50	0.015	0.03	0.02	0.03
Relative permittivity, ε_r	14.90	13.60	13.60	9.00	9.00	9.00
Band gap, E_g (eV)	1.41	1.19	1.34	3.60	3.20	3.20
Electron affinity χ (eV)	4.40	4.50	4.50	4.15	4.50	4.50
Density of states in conduction band, N_C (cm^{-3})	2.2×10^{18}	6.8×10^{17}	6.8×10^{17}	2.2×10^{18}	3.10^{18}	3.10^{17}
Density of states in valence band, N_V (cm^{-3})	1.8×10^{18}	1.5×10^{19}	1.5×10^{19}	1.8×10^{19}	1.7×10^{19}	1.7×10^{19}
Electron mobility, μ_n (cm^2/Vs)	100	100	10	100	100	100
Hole mobility, μ_p (cm^2/Vs)	50	50	1,25	25	31	31
Donor concentration, N_d (cm^{-3})	0	0	0	10^{18}	10^{18}	10^{20}
Acceptor concentration, N_a (cm^{-3})	10^{19}	6.10^{17}	6.10^{17}	0	0	0

5. Result and Discussion

We sought to optimize the thickness of the $MoSe_2$ interfacial layer, inevitably produced between the absorber layer and the rear Mo contact, by varying its thickness from 0.01 to 0.10 μm in order to observe its impact on the electrical performance of the cell (**Figure 5**).

The electrical performance of the cell improves as the thickness of the $MoSe_2$ interfacial layer increases **Figure 5**. The efficiency of the cell increases to about 24.6% for an interfacial layer thickness of 0.03 microns. For higher thicknesses, it remains almost constant with a slope of 0.05% per micron. In fact, too wide a thickness of the $MoSe_2$ leads to photogeneration of the carriers in this region and therefore extends the width of the region p (**Figure 5(c)**). Besides being in agreement with experimental studies, an excessive thickness of this layer could affect the FF (**Figure 5(b)**), [11] and consequently the performance of the cell. The thickness of the $MoSe_2$ layer must therefore be carefully controlled.

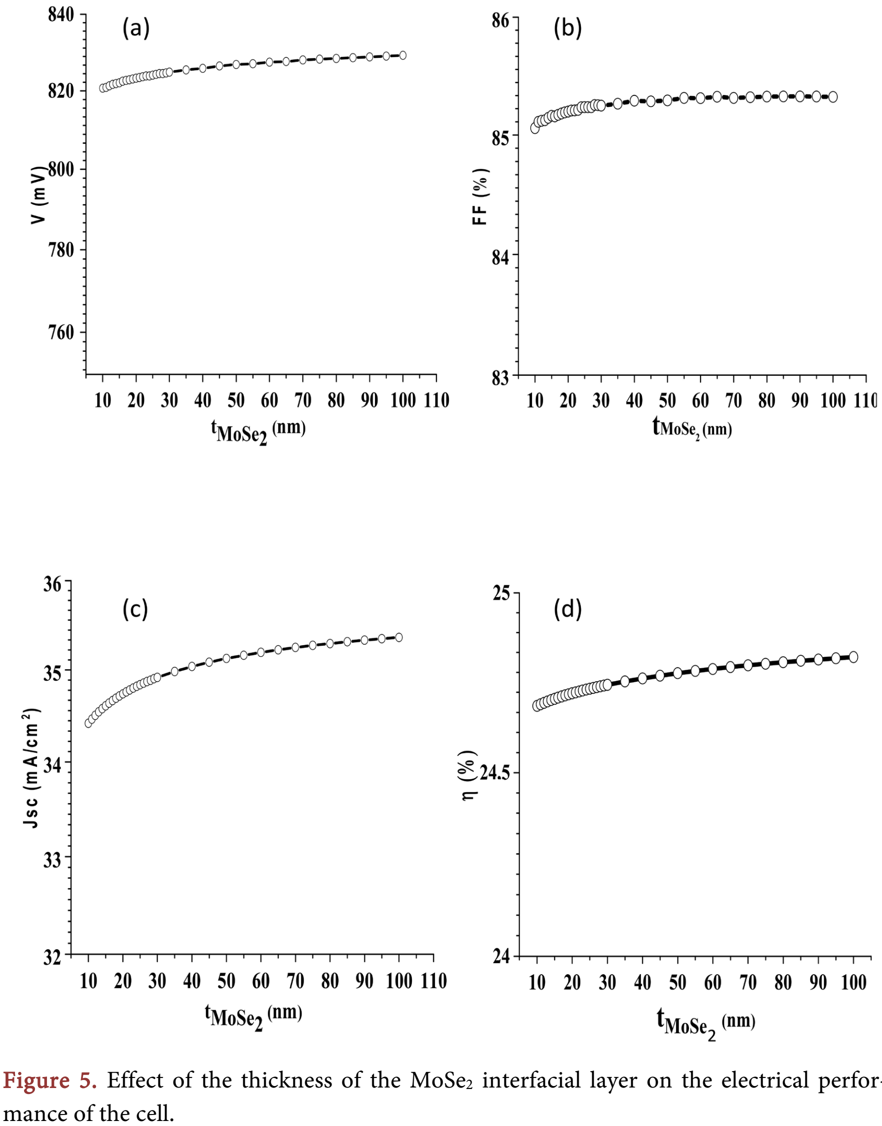

Figure 5. Effect of the thickness of the $MoSe_2$ interfacial layer on the electrical performance of the cell.

The quantum efficiency of the cell with the $MoSe_2$ interfacial layer and the $CIGSe_2$ absorber layer, with respective thicknesses of 0.03 µm and 1.5 µm, was evaluated (**Figure 6**). For wavelengths between 300 nm and 600 nm which constitute more than half of the visible, the quantum efficiency increases rapidly. In fact, this portion of the solar radiation is mostly absorbed in the first layers of the cell, in particular in the absorber layer.

5.1. Influence of the Thickness of the $CIGSe_2$ Layer

To observe the effect of the CIGSe absorber layer on the electrical performance of the cell with the 0.03 µm thick $MoSe_2$ interfacial layer, we varied the thickness of the $CIGSe_2$ from 0.1 to 10 µm. The performance of the cell is considerably better from the first microns of the CIGSe layer, that is to say for the ultra-fine cells of $CIGSe_2$. When the thickness of this layer is greater than 1.5 µm, the electrical performance of the cell is practically constant (**Figure 7(a)**, **Figure 7(c)** and **Figure 7(d)**).

In contrast, **Figure 7(b)** shows a slight decrease in the form factor when the thickness of the $CIGSe_2$ is greater than 1.5 µm. As we can see, the beneficial strengths of the $MoSe_2$ interfacial layer are observable for ultrafine layers of $CIGSe_2$.

5.2. Band Structure and Effect of the $MoSe_2$ Layer on the Schottky Barrier at the Rear Contact Interfaces

A study on the band diagram at the interface of the back contact with the $MoSe_2$ interfacial layer using the AFORS-HET digital simulation software is shown in **Figure 8**. The input parameters (**Table 1**), show that $e\phi CIGSe_2 > e\phi Mo$ which means that the $CIGSe_2$/Mo contact is of the Schottky type. Indeed, we witness in more detail a $CIGSe_2$/$MoSe_2$/Mo contact with two interfaces: $CIGSe_2$/$MoSe_2$ which is an SS contact and $MoSe_2$/Mo which is an MS contact whose nature generally depends on the types of doping, on the offsets, bands (conduction and valence) and work out of the materials involved.

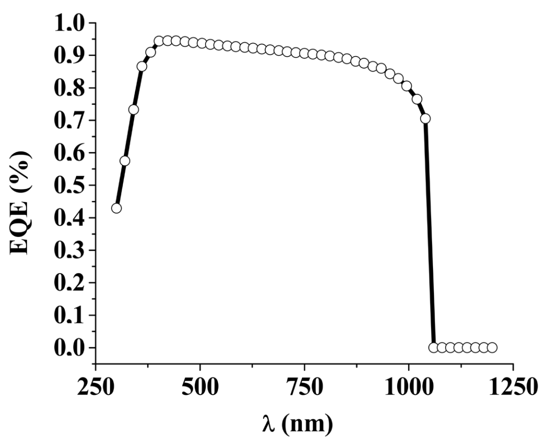

Figure 6. Cell quantum yield with 0.03 micron $MoSe_2$ interfacial layer.

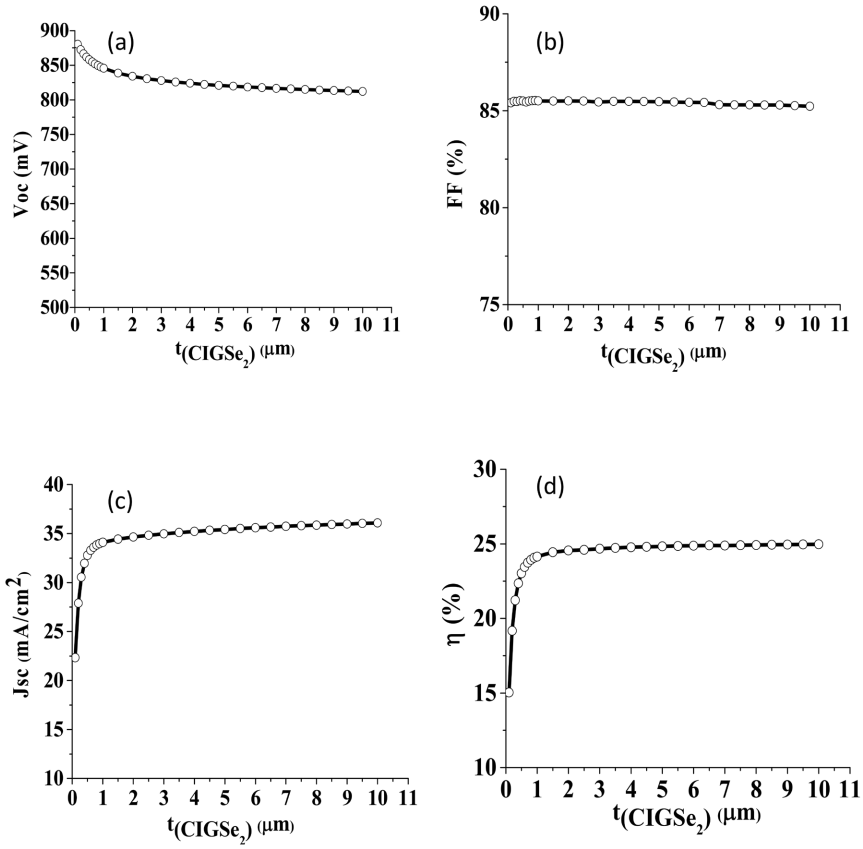

Figure 7. Effect of the thickness of the CIGSe absorber layer with $MoSe_2$ interfacial layer of 0.03 μm thickness.

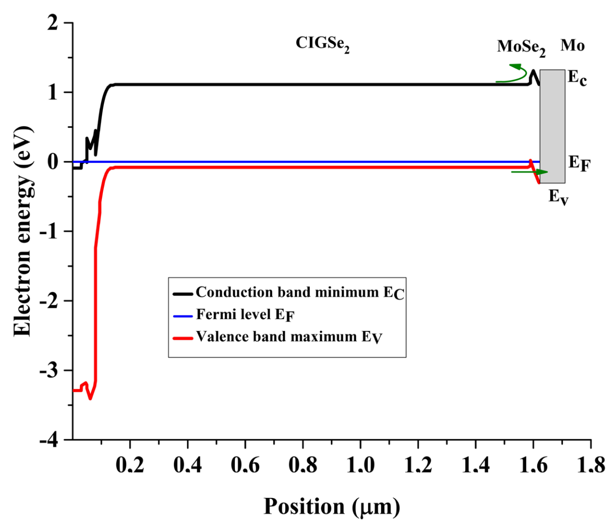

Figure 8. Band structures of the cell with the $MoSe_2$ interfacial layer contacting $CIGSe_2$/Mo.

For the $CIGSe_2$/$MoSe_2$ contact, the $MoSe_2$ gap greater than that of the $CIGSe_2$ causes a spike at the level of the conduction band which pushes the electrons towards the $CIGSe_2$/ZnS where the probability of collection is high and the Na concentration improves the diffusion of the holes towards the rear contact.

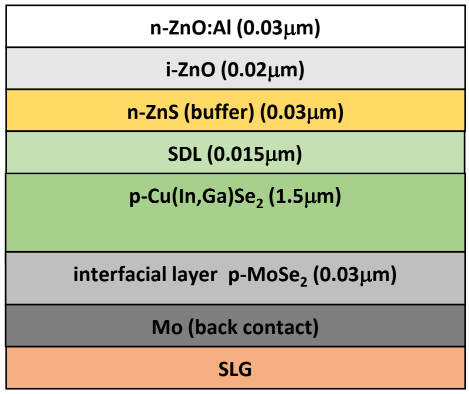

Figure 9. Thickness of the layers of the cell obtained after the simulation.

Table 2. Electrical parameters of the cell obtained after the simulation.

Thickness Of $CIGSe_2$ (μm)	Thickness Of interfacial layer $MoSe_2$ (μm)	V_{oc} (mV)	FF (%)	J_{sc} (mA/cm^2)	η %
1.50	0.03	829.20	85.40	35.15	24.60

For the $MoSe_2$/Mo contact, in addition to avoiding the recombinations of electrons at the back contact, the Na concentration of the $MoSe_2$ layer causes a curvature towards the Fermi level thus allowing the passage of the holes by tunneling effect.

The $MoSe_2$ interfacial layer therefore transforms the Schottky $CIGSe_2$/Mo contact into a quasi-ohmic contact.

5.3. Structure of the Simulated CIGS Solar Cell with a $MoSe_2$ Layer at the Rear Contact Interface

After optimization of all the cell layer properties, the thickness of the $CIGSe_2$ layer is reduced to 1.5 μm and an additional very thin layer of $MoSe_2$ tunnel layer of 0.03 μm thickness is formed between the region of the cell. $CIGSe_2$ absorber and back contact Mo. The proposed ultra-thin structure of the CIGS solar cell after simulation is shown in **Figure 9** and its electrical parameters obtained in **Table 2**.

6. Conclusion

Various experimental works reported have demonstrated the presence of a thin layer of $MoSe_2$ at the $CIGSe_2$/Mo contact interface. This layer of $MoSe_2$ transforms the nature of the Schottky $CIGSe_2$/Mo contact into a quasi-ohmic nature under a tunnel effect. Due to a strong p-doping, the thin layer of $MoSe_2$ allows a better transport of the majority carriers, by tunneling them from $CIGSe_2$ to Mo. In addition, the band gap of $MoSe_2$ is wider than that of the absorbent layer $CIGSe_2$, so that an electric field is generated nearby at the back surface. The presence of this electric field reduces the recombination of carriers at the interface. Under these conditions, we examined the performance of the cell with $MoSe_2$ layer. When the thickness of the $CIGSe_2$ absorber is between 3.5 µm and 1.5 µm, the efficiency of the cell with an interfacial layer of $MoSe_2$ remains almost constant, around 24.6%, while according to the literature that of solar cell without $MoSe_2$ is order at 23.4%. In addition, a Schottky barrier height greater than 0.45 eV severely affects the fill factor and open circuit voltage of solar cell with $MoSe_2$ interface layer compared to solar cell without $MoSe_2$.

Conflicts of Interest

The authors declare no conflicts of interest regarding the publication of this paper.

References

[1] Sylla, A. (2018) Modélisation et simulation d'une cellule solaire en couches minces à base de CuIn1-xGaxSe₂ utilisant un tampon Zn(O, S). Université Félix Houphouët Boigny.

[2] Green, M.A., Emery, K., Hishikawa, Y., Warta, W. and Dunlop, E.D. (2016) Solar Cell Efficiency Tables (Version 48). *Progress Photovoltaics Journal*, **24**, 905-913. https://doi.org/10.1002/pip.2788

[3] Friedlmeier, T.M., *et al.* (2015) Improved Photocurrent in $Cu(In,Ga)Se_2$ Solar Cells: From 20.8% to 21.7% Efficiency. *IEEE 42nd Photovoltaic Specialist Conference* (*PVSC*), New Orleans, LA, 14-19 June 2015, 1-3. https://doi.org/10.1109/PVSC.2015.7356152

[4] Solibro Press Release. (2014) Solibro Beats World Record for Solar Cells. Dated 12 June.

[5] Solar Frontier Press Release. (2015) Solar Frontier Achieves World Record Thin-Film Solar Cell Efficiency: 22.3%. 8 December. https://doi.org/10.1016/j.jpcs.2005.09.087

[6] Gloeckler, M. and Sites, J.R. (2005) Band-Gap Grading in Cu(In,Ga)Se Solar Cells. *Journal of Physics and Chemistry of Solids*, **66**, 1891-1894. https://doi.org/10.1016/j.solener.2011.08.003

[7] Saji, V.S., Choi, I.-H. and Lee, C.-W. (2011) Progress in Electrodeposited Absorber Layer for $CuIn(1-x)GaxSe_1$ (CIGS) Solar Cells. *Solar Energy*, **85**, 2666-2678. https://doi.org/10.1016/j.egypro.2010.07.009

[8] Decocka, K., Lauwaerta, J. and Burgelmana, M. (2010) Characterization of Graded CIGS Solar Cells. *Energy Procedia*, **2**, 49-54.

[9] Varache, R. (2012) Développement, caractérisation et modélisation d'interfaces pour cellules solaires à haut rendement à base d'hétérojonctions de silicium. Thèse de Doctorat, Universite Paris-Sud.

[10] Paulson, P.D., Birkmire, R.W. and Shafarman, W.N. (2003) Optical Characterization of CuIn(1−x)GaxSe Alloy Thin Films by Spectroscopic Ellipsometry. *Journal of Applied Physics*, **94**, 879-888.

[11] Raquel, C., *et al.* (2010) Cu Deficiency in Multi-Stage Co-Evaporated $Cu(In,Ga)Se_2$ for Solar Cells Applications: Microstructure and Ga In-Depth Alloying. *Acta Materialia*, **58**, 3468-3476.